PROPERTY MEASUREMENT IN NATURALLY FRACTURED DEVONIAN SHALE CORES USING A NEW PRESSURE PULSE METHOD

Xiuxu Ning*, Jin Fan, Stephen. A. Holditch,
and W. John Lee, Texas A&M University

ABSTRACT

This paper presents the application of a new laboratory technique to measure the distinct properties of the matrix and the fractures in naturally fractured, low permeability cores. The new technique can be used to determine (1) the porosity of the matrix, (2) the permeability of the matrix, (3) the effective permeability of the fractures, and (4) the effective width of the fractures.

The basic analytical solution that models pressure pulse test in a naturally fractured core has been published in a previous paper[1]. In this paper, we present the techniques for modifying the analytical solutions when (1) the core sample contains multiple fractures, and (2) the core sample has a single fracture away from the center of the core. We also present a new set of analytical solutions that take into account the gas leaks from the equipment during the pressure pulse test. Another way to solve the leaking problem is to compensate the pressure transient data for the pressure decrease due to leaks from the system. A numerical leak compensation method is demonstrated.

The new laboratory technique has been used to analyze more than twenty naturally fractured Devonian Shale cores from two wells. The results of measurements show that the gas filled matrix porosity ranges from 1.7% to 5.4%; the permeability of the matrix ranges from 1.9×10^{-9} to 5.5×10^{-8} millidarcies; and the fracture conductivity ranges from 6.65×10^{-6} to 1.03 millidarcy-inches. The distinctive properties of the matrix and the fractures can be used in reservoir simulation models to predict the behavior of the naturally fractured reservoirs in the Devonian Shale formation.

INTRODUCTION

The properties of the matrix and the fractures in naturally fractured reservoirs are the key parameters used in reservoir simulation models to predict the performance of naturally fractured reservoirs. However, laboratory techniques for measuring the distinctive properties of the matrix and the natural fractures were not available until recently.

In 1990, Kamath *et al.*[2] first showed that the pressure transient behavior of a pressure pulse test in a fractured core was different from that in a homogeneous core if the equipment is properly designed. They calculated the pressure responses for pressure pulse tests in

* Currently with Schlumberger Dowell

homogeneous and fractured cores with a finite difference model. They also conducted measurements with an artificially split sandstone sample and matched the experimental data with numerical solutions to obtain the fracture and matrix properties.

Ning *et al.*[1] presented a set of analytical solutions describing the pressure transient behavior of a pressure pulse test in a naturally fractured core. They constructed laboratory equipment used to perform pressure pulse tests in naturally fractured, low permeability cores. They also developed an automatic history matching program to analyze the laboratory measured pressure transient data using the analytical solutions.

In this paper, we present a new set of analytical solutions for pressure pulse test in naturally fractured cores taking into account the leaks from the equipment during the test. We will discuss the modification of the physical model to represent real core samples. We will also present a numerical leak compensation method to correct the pressure transient data for leaks in the equipment. We have analyzed over twenty naturally fractured Devonian Shale core samples using the new pressure pulse method. The results of measurements with twelve cores from the FMC#69 well have been presented by Ning *et al.*[1]. In this paper, we will present the results measured in eleven Devonian Shale cores from the FMC#78 well.

THEORY

Fig. 1 is a schematic diagram for the pressure pulse test in a naturally fractured core. The core sample is loaded in the rubber sleeve of a core holder so that a confining pressure can be applied around the core and a pore pressure can be applied inside the core. There is an upstream volume (V_u) at one end and a downstream volume (V_d) at the other end of the sample.

To conduct a pressure pulse test, a confining pressure (p_c) is applied to the outside of the core and a system pressure (p_i) is applied in the upstream volume, the downstream volume and the pore space of the core. The three volumes are filled with gas and the pressure in the system is allowed to reach equilibrium before the test. To start the test, a certain amount of gas is quickly injected into V_u to generate a pressure pulse in the upstream volume. As gas flows from the upstream volume through the fracture to the downstream volume, the pressure in V_u decreases and the pressure in V_d increases. Gas also flow into the matrix from the upstream volume, the downstream volume, and the fracture. The pressures in the upstream volume and the downstream volume are recorded as a function of time and analyzed afterwards to determine the properties of the matrix and the fracture.

Physical Models

When deriving the analytical solutions, Ning *et al.*[1] simplified the cylindrical core sample into a parallelepiped. They assumed that the core sample had a single fracture running through the center. However, real core samples often have either a single fracture away from the center of the

core or multiple fractures running through the core. As such, the mathematical models must be modified to describe the pressure pulse test in real core samples.

When determining the dimensions of the simplified model to represent a real core sample, we need to follow the following rules:

1. The ratios of the matrix volume, the fracture volume, and the downstream volume to the upstream volume should remain unchanged so that the material balance in the system always holds; and

2. The cross sectional area perpendicular to the direction of gas flow should remain unchanged so that the rate of gas flow across a certain surface always remains the same.

Case 1: A Single Fracture Near the Center of the Core Sample

If the real core sample has a single fracture near the center, we can represent it using a simplified model with a fracture running through the center as shown in Fig. 2. To comply with the rules stated above, the length of the simplified model will be the same as that of the core sample. The fracture width (h_f) will remain the same. The width of the simplified model (W) will be the same as the length of the fracture (W_f) on the cross section,

$$W = W_f. \tag{1}$$

The cross sectional area of the simplified model will be the same as that of the core sample,

$$A = \frac{\pi}{4} D^2 = W \times (h_m + h_f). \tag{2}$$

Then, the thickness of the matrix in the simplified model is

$$h_m = \frac{A}{W} - h_f. \tag{3}$$

Case 2: A Single Fracture Near the Edge of a Core Sample

In case the fracture is located very near to the edge of the core, we can simplify the sample into a parallelepiped with a fracture at the edge, as shown in Fig. 3. The dimensions of the simplified model in this case can be determined in the same way as in Case 1. The analytical solutions derived for the model discussed in Case 1 can be used to describe the pressure pulse test

in this model with slight adjustments. All we need to do is to substitute h_m and h_f with $2h_m$ and $2h_f$ respectively when calculating the dimensionless parameters used in the analytical solutions.

Case 3: Multiple Parallel Fractures in a Core Sample

When a core sample has multiple parallel fractures running through it, we can still simplify the sample into a parallelepiped as illustrated in Fig. 4. Suppose the core has n fractures with lengths of W_{f1}, W_{f2}, ... W_{fn}. We assume that the fractures are evenly distributed in the core sample and have the same conductivity. The matrix is divided into $n+1$ slabs by the fractures. The outer surfaces of the two slabs at the top and the bottom are no flow boundaries. The surface at the middle of each slab is also a no flow boundary. We can imaginarily slice the core sample along the no flow boundaries and connect the pieces side by side to form a parallelepiped as shown in Fig. 4.

The length of the simplified model will be the same as that of the core sample. The fracture width in the simplified model will be the average width of all fractures in the core sample. The width of the simplified model is equal to the total length of the fractures, i. e.:

$$W = \sum_{i=1}^{n} W_{fi} \,. \tag{4}$$

The height of the simplified model can be calculated using Eq. 3.

According to the simulation study conducted by Hopkins *et al.*[3], the position of the fracture in the core sample does not substantially affect the shape of pressure transient curves. Therefore, the simplified models can be used to represent real core samples in the cases discussed above without creating significant errors.

Analytical Solutions

Ning *et al.*[1] presented a set of analytical solutions to model the pressure pulse test in a fractured core. They assumed that the gas does not leak from the system during the pressure pulse test. However, we can never eliminate the leaking problem completely in practice, especially when working with high pressure helium. Because the matrix permeability of some naturally fractured formation can be very low (for example, the Devonian Shale formation has a matrix permeability in the order of 10^{-9} md), a pressure pulse test can last more than 12 hours with our current equipment. Any small leak in the system during the test can cause significant error in the pressure transient data. For example, if the leaking rate from the upstream and the downstream volume is 0.01 psi per minute, the pressure deviation during the test can be 7.2 psi in 12 hours. This is a significant error when compared with a typical pressure pulse of 35 psi and a typical final equilibrium pressure of 15 psi.

To solve the problem, we have developed two approaches to compensate for the leaks. One approach is called the **analytical compensation method**. The other approach is called the **numerical compensation method.** In the analytical compensation method, we have derived a new set of analytical solutions which takes into account the leaks from the upstream volume and the downstream volume during the pressure pulse test.

Analogous to Darcy's law, we assume that the volumetric leaking rate (q_l) from the upstream volume and the downstream volume is proportional to the difference between the system pressure and the atmospheric pressure (p_a),

$$q_{lj} = \frac{2c_j}{\mu}(p_j - p_a), \qquad j = u, d, e, \qquad (5)$$

where, c_u, c_d, and c_e are constants we call the **leaking coefficients** for the upstream volume, the downstream volume, and the late time equivalent volume respectively. The mass leaking rate can be written as

$$\begin{aligned} \rho q_{lj} &= \frac{(P_j + P_a)M}{2ZRT}\frac{2c_j}{\mu}(p_j - p_a) \\ &= \frac{Mc_j}{\mu ZRT}\left(p_j^2 - p_a^2\right) \\ &\approx \frac{Mc_j}{RT}(p_{pj} - p_{pa}), \\ & \qquad j = u, d, e. \qquad (6) \end{aligned}$$

To obtain the analytical expressions for the pressure transient behavior in the upstream and the downstream volume, we need to write a diffusivity equation in the fracture, a diffusivity equation in the matrix, and a material balance equation in the upstream volume and the downstream volume respectively. The material balance equations take into account the mass leaking rates calculated using Eq. 6. Since the boundary conditions of the differential equations are related with each other, we need to solve the system of differential equations simultaneously to obtain the analytical solution. Detailed derivations have been documented by Ning[4]. The final form of the analytical solution that accounts for the leaks from the upstream volume and the downstream volume is shown as follows:

Early time dimensionless pseudopressure in upstream volume:

$$\overline{p_{pDu}} = \frac{\frac{B\xi_u}{\alpha} + (B\delta_u - A\delta_d)\frac{p_{pDa}}{u}}{BC - A^2}, \tag{7}$$

Early time dimensionless pseudopressure in downstream volume:

$$\overline{p_{pDd}} = \frac{\frac{A\xi_u}{\alpha} + (A\delta_u - C\delta_d)\frac{p_{pDa}}{u}}{BC - A^2}, \tag{8}$$

where,

$$A = \frac{\sqrt{f(u)}}{sh\sqrt{f(u)}} + \frac{\sqrt{\omega\xi_m\lambda u}}{sh\sqrt{\frac{\omega\xi_m u}{\lambda}}}, \tag{9}$$

$$B = \frac{\sqrt{f(u)}}{th\sqrt{f(u)}} + \frac{\sqrt{\omega\xi_m\lambda u}}{th\sqrt{\frac{\omega\xi_m u}{\lambda}}} + \frac{\gamma\xi_d u}{\alpha} - \delta_d, \tag{10}$$

$$C = \frac{\sqrt{f(u)}}{th\sqrt{f(u)}} + \frac{\sqrt{\omega\xi_m\lambda u}}{th\sqrt{\frac{\omega\xi_m u}{\lambda}}} + \frac{\xi_u u}{\alpha} + \delta_u, \tag{11}$$

$$f(u) = \sqrt{\omega\xi_f\lambda\eta u}\cdot th\sqrt{\frac{\omega\xi_f u}{\lambda\eta}} + u\xi_f, \tag{12}$$

and δ's are dimensionless leaking coefficient defined as

$$\delta_j = \frac{Lc_j}{Wk_f h_f}, \qquad j = u, d. \tag{13}$$

Late time dimensionless pseudopressure in the equivalent volume:

$$\overline{p_{pDe}} = \frac{\frac{\zeta \xi_e p_{ppDe}}{\kappa_l \lambda \eta} + \frac{\varepsilon p_{pDa}}{u}}{\varepsilon + \frac{\xi \xi_e u}{\kappa_l \lambda \eta} + \sqrt{\frac{\omega \xi_m u}{\lambda \eta}} th\left(\sqrt{\frac{\omega \xi_m u}{\lambda \eta}} \kappa_h\right)}, \qquad (14)$$

where

$$\varepsilon = \frac{h_m c_e}{4 W k_f h_f}. \qquad (15)$$

For detailed definitions of the dimensionless variables refer to reference 4.

Eqs. 7 through Eqs. 15 will revert to the analytical solutions presented by Ning *et al.*[1] if we set the leaking coefficients (c_u, c_d and c_e) to zero. The leaking coefficients in the above equations can be calculated from the pressure leaking rate using the following equation:

$$c_j = \frac{\mu V_j}{p_j^2 - p_a^2} \frac{dp_j}{dt}, \qquad j = u, d, e. \qquad (16)$$

The pressure leaking rate can be determined in the laboratory.

Numerical Leak Compensation Method

The numerical leak compensation method is a simpler way to solve the leaking problem. In this approach, we first determine the pressure leaking rate during a pressure pulse test and then correct the original pressure transient data to compensate for the leaks.

There are two ways to determine the leaking rate. One way is to measure the leaking rate after the system has reached the initial equilibrium and before the pressure pulse test. Another way is to calculate the leaking rate using the last few data points of the pressure pulse test. After the test has reached the final equilibrium pressure, any further pressure decrease in the system is caused by the leaks from the system.

Since the system pressure only changes approximately between 1000 and 1050 psi, we can assume that the pressure leaking rate is constant throughout the pressure pulse test. Then we can use the leaking rate measured before or after the test to calculate what the pressure transient data would have been if there had been no leak. The upstream and the downstream pressure data of the complete test are corrected as follows:

$$p_{jc}(t_i) = p_j(t_i) + \frac{dp_j}{dt} t_i, \qquad j = u, d. \qquad (17)$$

Fig. 5 presents a comparison between the original pressure transient data and the leak compensated data for a typical Devonian Shale core sample. The squares represent the original data and the solid lines represent the corrected data. We can see that it would be impossible for us to match the original data with the analytical solutions without making corrections for the leak.

LABORATORY EQUIPMENT

We have designed and constructed laboratory equipment to conduct pressure pulse measurements in either fractured or homogeneous, low permeability cores. Fig. 6 is a schematic diagram of our laboratory equipment. The equipment includes the following main components:

1. An insulation chamber that houses the critical components to prevent the test from being affected by the changes in ambient temperature;

2. A core holder that holds core samples during a pressure pulse test;

3. A gas accumulator that supplies gas to the system;

4. A reference pressure accumulator that provides a constant reference pressure for the differential pressure transducers;

5. A pressure regulator that controls the system pressure, and generates the pressure pulse in the upstream volume at the beginning of a test;

6. A hydraulic pump that provides the confining pressure to the core holder;

7. Tubing and valves to connect the different components;

8. Two differential pressure transducers to measure the differential pressures in the upstream volume and the downstream volume relative to the reference pressure;

9. A reference pressure transducer to measure the pressure in the reference volume;

10. A confining pressure transducer to measure the pressure of the confining fluid;

11. A thermal couple to measure the temperature in the upstream volume; and

12. A data acquisition system including a data acquisition board and a personal computer.

According to the numerical simulation study conducted by Hopkins *et al.*[3], the upstream and downstream volumes must be on the same order of magnitude as the pore volume of the sample in order for fractured cores to exhibit heterogeneous pressure transient behavior during the pressure pulse test. Our laboratory equipment has an upstream volume of 3.4 cc and a downstream volume of 2.0 cc which satisfies the requirement.

RESULTS OF MEASUREMENTS

To determine the properties of a core sample, we first measure the dimensions of the sample and identify the number and the positions of the fractures. We then load the sample into the equipment and conduct pressure pulse test with it. The pressure leaking rate is determined using the last few points of the pressure transient data. The leaking rate is used to correct the raw pressure transient data and the corrected data are then analyzed using an automatic history matching program. The history matching program matches the laboratory measured pressure transient data using analytical solutions to determine (1) the porosity of the matrix, (2) the permeability of the matrix, (3) the effective permeability of the fractures, and (4) the effective width of the fractures[1].

The Devonian Shale formation is a naturally fractured, extremely low permeability gas formation in the Appalachian Basin. It is considered a large source of natural gas in the eastern part of the United States. Using the laboratory technique developed in this research, we have performed measurements with over twenty naturally fractured Devonian Shale cores. The results of measurements with twelve cores from the FMC#69 well were reported by Ning *et al*[1]. In this paper, we present the results of measurements with eleven new Devonian Shale core samples from the FMC#78 well located in eastern Kentucky.

Detailed discussions for each core sample has been documented by Fan[5]. As an example, core No. 1 from well FMC#78 is a finely laminated shale with three major fractures that are parallel with the lamination. Fig. 7 presents the match between the experimental data and the analytical solution for this sample. Dimensionless pressures in the upstream volume and the downstream volume are graphed as functions of time. The squares are experimental data and the solid lines are the analytical solution. As we can see, the upstream pressure decreases and the downstream pressure increases at the early time of the pressure pulse test. After about 300 seconds, the pressures in the upstream volume and the downstream volume converge to the same value. This is because gas flows from the upstream volume to the downstream volume through the fractures. Then, as gas flows into the matrix from the upstream volume, the downstream volume, and the fracture, the pressures in the upstream volume and the downstream volume decrease together until they reach the final equilibrium. Fig. 7 shows that the experimental data and the analytical solutions match well. Using the history matching program developed by Ning *et al*[1], the matrix porosity is determined to be 1.7%; the matrix permeability is 1.68×10^{-8} md; the average fracture conductivity is 6.55×10^{-4} md-in; the average effective fracture permeability is 28.7 md; and the average effective fracture width is 0.58 microns.

Table 4.1 summarizes the results of measurements with eleven Devonian Shale cores. The matrix gas porosity ranges from 1.7% to 5.4%; the permeability of the matrix ranges from 1.9×10^{-9} to 5.5×10^{-8} millidarcies; the fracture conductivity ranges from 6.65×10^{-6} to 1.03 millidarcy-inches; the effective permeability of the fractures ranges from 1.3 to 834.6 millidarcies; and the effective width of the fractures ranges from 0.13 to 3.15 microns.

Table 4.1 Results of Measurements with Devonian Shale Cores from Well FMC#78

Core No.	Matrix Porosity (%)	Matrix Permeability (md)	Fracture Permeability (md)	Fracture Width (μm)	Fracture Conductivity (md-in)	Number of Major Fractures
1	1.7	1.68E-8	28.7	0.58	6.55E-4	3
2	6.0	1.15E-8	175.5	1.44	9.95E-3	3 (artificial)
3	3.8	4.13E-9	16.7	0.45	2.96E-4	4
6	4.6	2.80E-8	386.0	2.14	3.25E-2	1
12	5.4	1.9E-9	80.1	0.97	3.06E-3	2 (artificial)
15	5.1	2.83E-8	834.6	3.15	0.103	1
17	4.3	2.95E-8	1.3	0.13	6.65E-6	2
21	4.4	5.5E-8	57.1	0.82	1.84E-3	2
27	2.5	1.68E-8	283.7	1.83	2.04E-2	1
28	4.8	1.12E-8	24.4	0.54	5.19E-4	3
30	3.8	3.51E-9	308.6	1.93	2.34E-2	2

Samples No. 2 and No. 12 did not have continuous natural fractures. When we tried to test these two cores in their original conditions, the tests failed because it took too long for the pressures in the upstream volume and the downstream volume to converge. To solve the problem, we artificially induced fractures in the samples and tested them again. The time needed to test a sample with fractures (natural or artificial) is much shorter than the time needed to test a homogeneous sample with the same matrix permeability. These examples demonstrate that when a homogeneous core has a permeability too low to be measured, we can purposely crack the core and test the artificially fractured sample using the new pressure pulse method developed in this research.

CONCLUSIONS

1. A new pressure pulse method has been developed to determine the distinctive properties of the matrix and the fractures in naturally fractured, low permeability cores. The new method has been used to analyze over twenty naturally fractured Devonian Shale core samples.

2. New analytical solutions for pressure pulse test in a fractured core have been derived. The solutions take into account the gas leaks in the equipment during the test.

3. The analytical solutions derived for a physical model with a fracture in the center can be applied with proper modifications when the core sample contains either multiple fractures or a single fracture away from the center of the core.

4. A numerical leak compensation method has been developed and applied to correct the pressure transient data for leaks during a pressure pulse test which can significantly affect the pressure transient data when testing low permeability cores

5. For the eleven cores from the FMC#78 well, the matrix gas filled porosity ranges from 1.7% to 5.4%; the permeability of the matrix ranges from 1.9×10^{-9} to 5.5×10^{-8} millidarcies; and the fracture conductivity ranges from 6.65×10^{-6} to 1.03 millidarcy-inches.

NOMENCLATURE

A = Cross sectional area of core sample, ft^2, or Dimensionless group as defined in Eq. 9
B = Dimensionless group as defined in Eq. 10
C = Dimensionless group as defined in Eq. 11
c_d = Leaking coefficient for downstream volume, scf/sec·cp/psia
c_e = Leaking coefficient for equivalent volume, scf/sec·cp/psia
c_u = Leaking coefficient for upstream volume, scf/sec·cp/psia
D = Diameter of core sample, ft
$f(u)$ = Dimensionless group in Laplace domain
h_f = Width of fracture, ft
h_m = Thickness of matrix, ft
k_f = Permeability of fracture, md
k_m = Permeability of matrix, md
L = Length of core sample, ft
M = Molecular weight of gas lbm/lb-mole
p_a = Atmospheric pressure, psia
p_c = Confining pressure, psia
p_d = Pressure in downstream volume, psia
p_{dc} = Corrected pressure in downstream volume, psia
p_e = Pressure in the equivalent volume, psia
p_i = Initial system pressure, psia
p_{pDa} = Dimensionless pseudopressure at atmospheric condition
$\overline{p_{pDd}}$ = Dimensionless pseudopressure in downstream volume in Laplace domain

$\overline{p_{pDe}}$ = Dimensionless pseudopressure in equivalent volume in Laplace domain

$\overline{p_{pDu}}$ = Dimensionless pseudopressure in upstream volume in Laplace domain

p_{pa} = Pseudopressure at atmospheric condition, psia^2/cp

p_{pe} = Pseudopressure in equivalent volume, psia^2/cp

p_{pm} = Pseudopressure in matrix, psia^2/cp

p_{ppDe} = Dimensionless pseudopressure pulse in the equivalent volume

p_{pu} = Pseudopressure in upstream volume, psia^2/cp

p_u = Pressure in upstream volume, psia

p_{uc} = Corrected pressure in upstream volume, psia

R = Gas constant, 10.732 psia·ft^3·/lb·mole·°R

T = Temperature, °R

t = Time, sec

u = Laplace variable, dimensionless

V_d = Downstream volume, ft^3

V_u = Upstream volume, ft^3

W = Width of physical model, ft

Z = Real gas compressibility factor, dimensionless

α = Fracture to upstream volume storativity ratio, dimensionless

δ_d = Dimensionless leaking coefficient in downstream volume

δ_u = Dimensionless leaking coefficient in upstream volume

ε = Dimensionless leaking coefficient in equivalent volume

γ = Downstream volume to upstream volume storativity ratio, dimensionless

η = Matrix aspect ratio squared, dimensionless

κ_l = Equivalent length to actual length ratio, dimensionless

κ_h = Equivalent height to actual height ratio, dimensionless

λ = Matrix to fracture transmissibility ratio, dimensionless

μ = Viscosity, cp

ρ = Gas density, lbm/scf

ω = Matrix to fracture storativity ratio as defined in Eq. 4.32, dimensionless

ξ_d = Downstream volume to reference viscosity-compressibility ratio, dimensionless

ξ_e = Equivalent volume to reference viscosity-compressibility ratio, dimensionless

ξ_f = Fracture to reference viscosity-compressibility ratio, dimensionless

ξ_m = Matrix to reference viscosity-compressibility ratio, dimensionless

ξ_u = Upstream volume to reference viscosity-compressibility ratio, dimensionless

ζ = Equivalent volume to fracture volume ratio, dimensionless

REFERENCES

1. Ning, X., Fan, J., Holditch, S. A., and Lee, W. J.: "The Measurement of Matrix and Fracture Properties in Naturally Fractured Cores," paper SPE 25898 presented at the SPE Rocky Mountain Regional / Low Permeability Reservoirs Symposium held in Denver, CO, April 12-14, 1993.

2. Kamath, J., Boyer, R. E., and Nakagawa, F. M.: " Characterization of Core Scale Heterogeneities Using Laboratory Pressure Transients," paper SPE 20575 presented at the 65th Annual Technical Conference and Exhibition of the Society of petroleum Engineers held in New Orleans, LA, Sep. 23-26, 1990.

3. Hopkins, C. W., Ning, X., and Lancaster, D. E.: " Reservoir Engineering and Treatment Design Technology - A Numerical Investigation of Laboratory Transient Pulse Testing for Evaluating Low Permeability, Naturally Fractured Core Samples," a Topical Report (Jan. - June 1991) submitted to Gas Research Institute, 8600 West Bryn Mawr Avenue, Chicago, IL 60631, GRI contract No. 5086-213-1446, Recipient's Accession No. GRI-91/0380.

4. Ning, X.:" The Measurement of Matrix and Fracture Properties in Naturally Fractured Low Permeability Cores Using a Pressure Pulse Method," Ph.D. dissertation, Texas A&M University, College Station, TX, (Dec. 1992)

5. Fan, J.:" Property Measurement and Correlation for Homogeneous and Naturally Fractured Low Permeability Cores," M. S. thesis, Texas A&M University, College Station, TX, (May 1993)

ACKNOWLEDGMENT

The authors acknowledge the Burlington Resources Foundation, GRI, and the Petroleum Engineering Department of Texas A&M University for the financial support to this research.

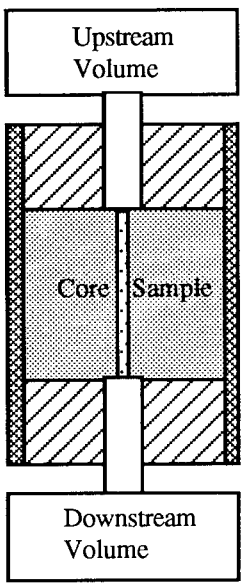

Figure 1 Schematic Diagram for Pressure Pulse Test

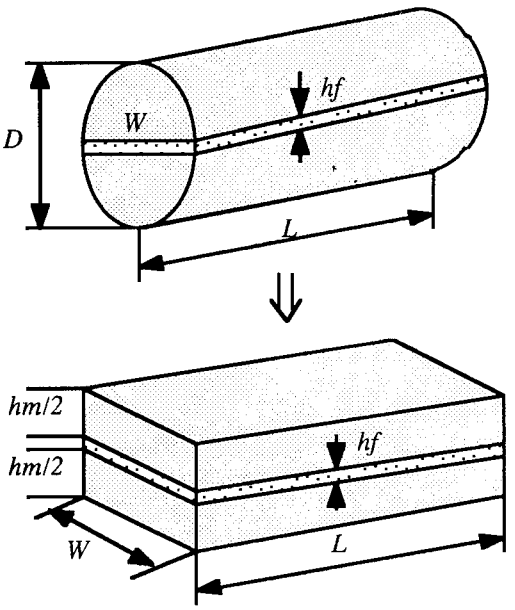

Figure 2 Simplified Model for a Fractured Core with a Fracture Near the Center

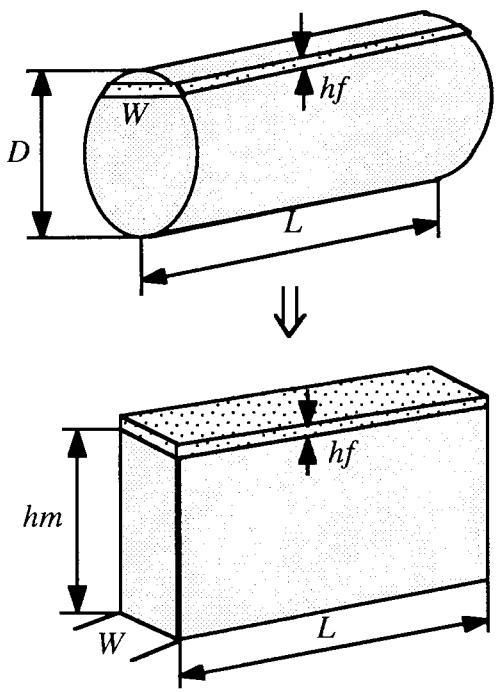

Figure 3 Simplified Model for a Core with a Fracture Near the Edge

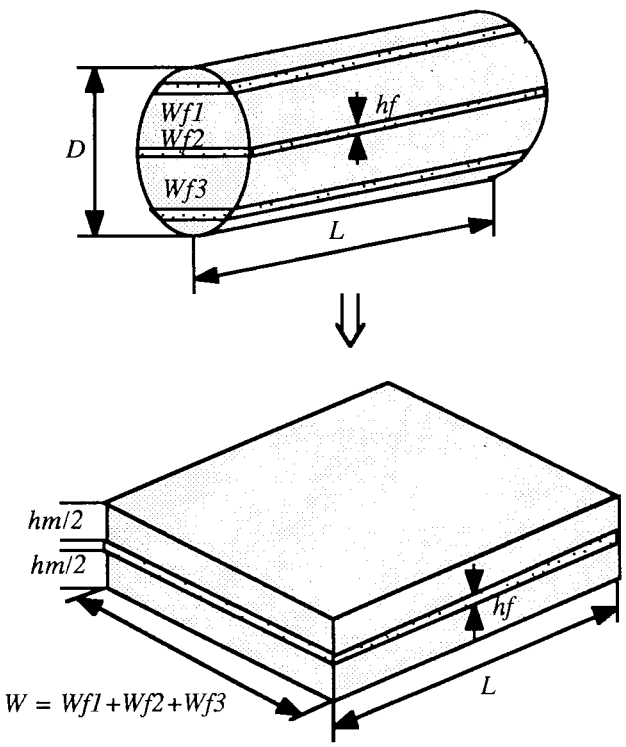

Figure 4 Simplified Model for a Core with Multiple Fractures

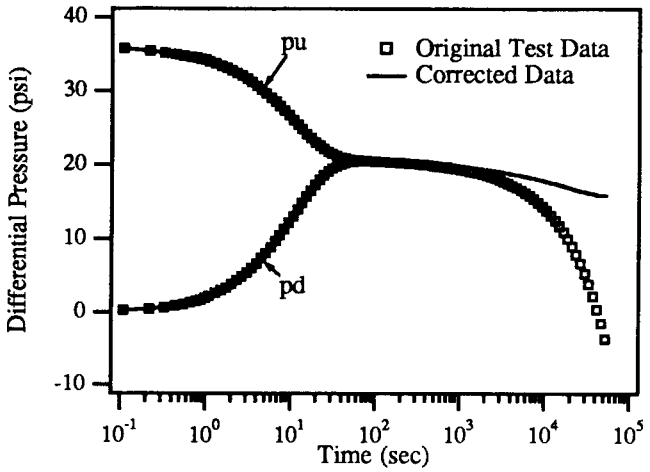

Figure 5 Comparison Between Original and Leak Compensated Pressure Transient Data

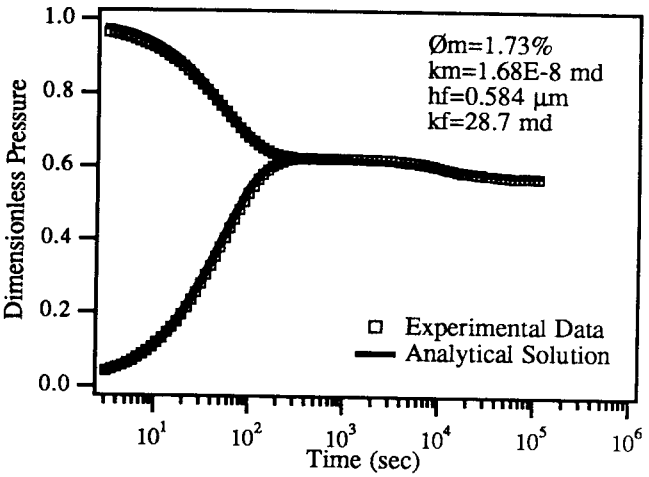

Figure 7 Match Between Experimental Data and Analytical Solution for Core No. 1

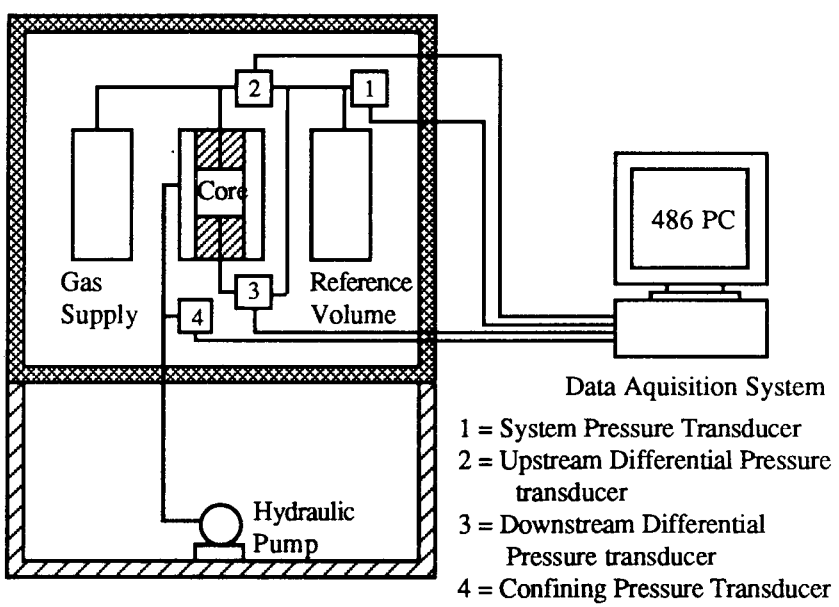

Figure 6 Schematic Diagram of the Laboratory Equipment